Mechanism for *c*-axis conduction in graphite intercalation compounds

R. Powers, A. K. Ibrahim, G. O. Zimmerman, and M. Tahar
Department of Physics, Boston University, Boston, Massachusetts 02215
(Received 9 February 1987; revised manuscript received 28 December 1987)

The four-probe technique is used to measure the *c*-axis resistivity of various stages of $FeCl_3$ acceptor graphite intercalated compounds. A comprehensive investigation of the resistivity behavior between room and liquid-helium temperatures for stages 2–5 and 9 and highly oriented pyrolytic graphite is presented. The data show a low-stage dependence where the resistivity increases with temperature, an intermediate stage where the temperature variation of the resistivity is small, and a high-stage dependence where the resistivity decreases with temperature. In our case, stage 5 plays the role of the intermediate stage. Stage 5 also exhibits the highest room-temperature resistivity. The *c*-axis resistivity data are analyzed in terms of the variable-range hopping-conduction model in parallel with band conduction.

INTRODUCTION

Because the $FeCl_3$ graphite intercalation compound (GIC) system is one of the earliest systems to have been investigated by numerous researchers, it often serves as a model GIC system. Within the past eight years systematic measurements of physical properties as a function of the GIC stage (the stage number denotes the number of graphite layers separating two successive intercalant layers) have revealed a number of interesting features. Thermal-conductivity measurements[1] have shown that the electronic thermal conductivity of the graphite bounding layers increases upon intercalation, whereas the lattice thermal conductivity decreases. Magnetic susceptibility measurements[2,3] on $FeCl_3$ indicate the existence of a low-temperature magnetic phase transition. Here we report the measurement of the *c*-axis resistivity of a series of stages of $FeCl_3$-GIC, and correlate the measurements with the hopping- and band-conductivity contributions in each stage. Previously, Metz and Hohlwein[4] have made a structural investigation using x-ray diffraction and conclude that the stacking of layers is disordered and under special circumstances, depending on the preparation condition, nearly periodic compounds can be produced. Infrared and Raman spectroscopy of $FeCl_3$-graphite[5] indicate in-plane compression within the graphite layers and that most of the effective charge is in the graphite bounding layers, with the rest of the charge distributed among the graphite interior layers.

In GIC's the electrical conductivity is one of the most promising physical quantities for which real applications might be found.[6] The in-plane and *c*-axis conductivities are among the properties most drastically charged by intercalation of acceptor and donor GIC's.[7,8] There is an anisotropy between the in-plane and *c*-axis resistivity which in some samples can be as high as 10^6,[9] where the in-plane resistivity is the smaller one. Because of the greater in-plane conductivity, which at times can become comparable to that of copper, most of the experimental and theoretical attention has been concentrated on the in-plane electrical properties.[10–14] To date there are two comprehensive measurements of the *c*-axis resistivity,[15,16] one on a donor and one on an acceptor system which show remarkable similarities in their temperature behavior.[17]

Phan, Fuerst, and Fischer[15] have measured the *c*-axis conductivity of potassium GIC and found that the high stages exhibited activated behavior, while the lower-stage compounds exhibited metallic-like conduction. The high stage activated behavior of the resistivity is attributed to the screening mechanism, while the low-stage metallic behavior is attributed to the intercalant band overlap.

The investigation of $SbCl_5$-GIC by Morelli and Uher[16] revealed a similar temperature behavior of the resistivity despite the fact that K-GIC is a donor compound while $SbCl_5$ is an acceptor compound. The fact that the low-stage compounds exhibit metallic-like conduction, was explained by a model based on defect-mediated short-circuiting channels along the *c* axis. In higher stages, however, a metal-insulator transition along the *c* axis is observed at low temperature and it was concluded that the conduction is essentially caused by thermally activated hopping.

Ohta, Kawamura, and Tsuzuku[18] have measured the temperature dependence of the *c*-axis resistivity of stages 1 and 2 ICl-GIC. Their data show an order-disorder transition at room temperature and an anisotropy of the order 10^3 for stage 1 and 10^4 for stage 2. Measurements of the *c*-axis resistivity for stage-2 $FeCl_3$-GIC by Issi *et al.*[19] indicate that the resistivity, after the subtraction of the residual part, has a T^2 dependence at low temperature, and a T dependence at high temperature. A compendium of various measurements of the *c*-axis resistivity for several GIC's, both donor and acceptor, was presented by McRae, Mareche, and Hérold.[17] It shows that there are some common characteristic signatures in the *c*-axis resistivity in both acceptor and donor GIC's.

Three theories have been advanced to explain the *c*-axis conductivity. The one by Sugihara[20] postulates a phonon and impurity assisted hopping mechanism which, in different stages and different temperature regimes gives rise to either a decrease or an increase of the resistivity

with temperature. Another theoretical treatment by Shimamura[21] also derives the two temperature dependences. Markiewicz[22] assumes that the c-axis conductivity takes place by means of very narrow bands which depend on the spacing between the graphite planes. Another factor which should be taken into account is the charge-screening mechanism which screens the charges in the intercalate layers and tends to confine most of the extra free carriers to graphite planes next to the intercalant.[23,24] In what follows, our data will be analyzed in terms of variable-range hopping conduction (VRHC), as described by Shklovskii and Efros,[25] in parallel with band conduction.

In this work, the c-axis resistivity measurements of the $FeCl_3$-graphite system using the conventional four-probe technique were stimulated by the investigation of the low-temperature anomaly of the magnetic susceptibility.[3] Contactless bridge measurements had been made on various stages and a peak in the susceptibility was observed at around 1.75 K. This peak was also noted in the out-of-phase component of the susceptibility which indicated a possible contribution from the resistivity of the sample.[26] For the sample orientation chosen in our measurements, this contribution would have been primarily from the c-axis resistivity. Thus it was decided to investigate the resistivity by means of independent measurements concurrently with the contactless bridge method.

EXPERIMENTAL

The $FeCl_3$-GIC samples were prepared using a standard two-zone furnace technique[6] where stage index was controlled by the temperature difference between the graphite host, highly oriented pyrolytic graphite (HOPG) and the $FeCl_3$ powder. The samples were in the form of thin rectangular plates of dimensions $1.5\times0.5\times0.1$ cm^3. Well-staged samples were achieved by controlling the pressure of Cl_2 gas inside the intercalation tube, as well as the partial pressure of $FeCl_3$ through rigid temperature control. After intercalation, the samples were characterized for identity and uniformity of staging using x-ray (001) diffraction. Only single stage, well-staged samples were used in the reported measurements. The x-ray diffractograms were also used to determine the c-axis repeat distance I_c after cycling the samples from room to liquid-helium temperature, and showed that the cycling did not affect this staging distance.

Most of the samples measured were characterized by means of the Mössbauer effect, details are reported in Refs. 3 and 27. In higher stage samples, where stage disorder is expected,[28] the Hendricks-Teller,[29] and Metz and Hohlwein[4] analysis technique were used to calculate the intensity, width, and location of the x-ray reflections. We find that our experimental x-ray data on the stage-9 samples reported in this paper are in good agreement with those calculated for the pure and well-staged stage 9. Although a small admixture of stage 10 cannot be excluded, this stage serves as an example of a high-stage sample.

For resistivity measurements, samples of approximate dimensions 0.3 mm by 5×5 mm^2 were cleaved from the intercalated samples, and the surfaces were cleaned by peeling the top and bottom layers using scotch tape. These dimensions were chosen primarily for convenience when mounting the samples in our sample holder, whereas optimal signal would have been obtained by minimizing the in-plane area while maintaining comfortable lead separation on the faces and maximizing the c-axis thickness. Because of the high in-plane conductivity relative to that of the c axis, nonuniform current injection would not be a problem. The leads were attached to the sample in the conventional four-probe configuration. Contacts were made on the sample using GC conductive silver print (GC Electronics). The samples were inserted in the axial slot of a phenolic rod which was then wrapped with mylar tape to insure that the sample did not move in the slot and that subsequent stress to the leads was minimized. The leads were attached to the main leads leading from the cryostat by wrapping and then glueing with silver print.

The temperature was measured using a calibrated silicon diode thermometer mounted close to the sample, and wired in a four-point contact configuration. The susceptibility and the c-axis voltages were measured simultaneously. The sample voltage was first read with zero current through the sample, then the sample current was set to 5 mA. This value of current was chosen as a tradeoff between low-power dissipation in the dewar and low noise in the signal. The voltage at 5 mA was taken and then the current was switched off. The sample voltage was then read again. The average of the zero current voltages, representing the thermal voltage in the junctions of the leads, was subtracted from the voltage at 5 mA. The sample resistance was calculated from this corrected voltage.

RESULTS AND ANALYSIS

The data plotted in Fig. 1 are the resistivity normalized to room temperature values versus temperature for stages 2, 3, 4, 5, and 9 of the $FeCl_3$-GIC, and HOPG. Because hysteretic behavior was observed for stage 9 (see discussion below) two sets of data appear for this stage, one for data taken when the sample was cooled, the other when it was warming up, the latter is denoted by 9r. Several features can be observed in the data. (1) For stage index less than 5 the temperature behavior of the resistivity is metallic-like (resistivity increases with temperature), and the resistivity saturates at low temperatures. The metallic behavior is most pronounced for stages 2 and 3 and less so for stage 4. (2) Note that for stage 5 the resistivity exhibits metallic-like behavior at high temperatures and crosses to activated behavior at low temperatures. (3) Observe that the highest stage sample, stage 9, exhibits activated behavior (resistivity decreases with temperature) throughout the entire range of temperatures shown. Although stage 9 exhibits activated behavior similar to HOPG as one would expect for higher stages, the increase in HOPG resistivity with temperature at low temperatures is not reproduced.

The absolute resistivity values at room temperature for stages 2, 3, 4, 5, and 9 of $FeCl_3$-GIC, and HOPG are listed in Table I. For comparison, the room-temperature

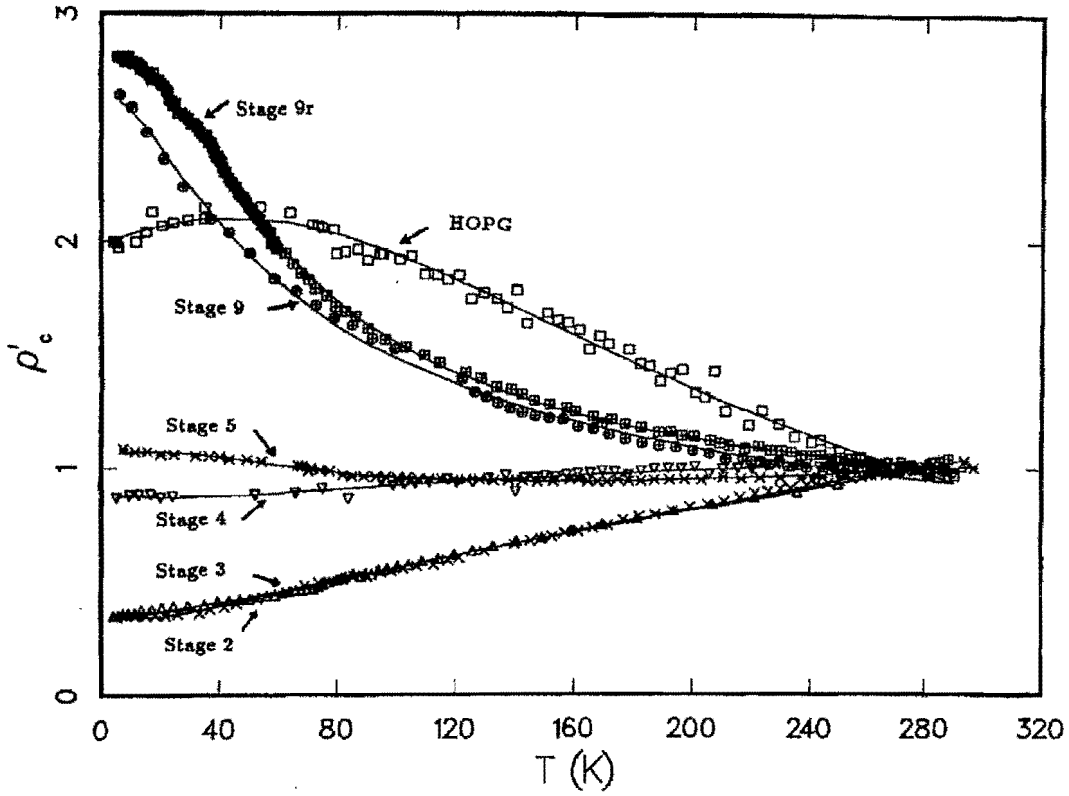

FIG. 1. The c-axis resistivity normalized to the room-temperature values vs temperature for stages-2, -3, -4, -5, and -9 $FeCl_3$-GIC's, and HOPG. The lines are fits to Eq. (4), see the text. $9r$ is the scan-up for stage 9.

resistivities measured by Morelli and Uher[16] on $SbCl_5$-GIC and Phan, Fuerst, and Fischer[15] on K-GIC, are also tabulated. As shown in the table, stage 5 has the largest resistivity among all stages and HOPG as well.

The absolute resistivity versus the inverse of the stage index is presented in Fig. 2 at 293, 77, and 4.2 K. At 293 and 77 K the peak in resistivity is at stage 5. This is, qualitatively, in agreement with the results of the magnetic measurements for the $FeCl_3$-GIC.[3] In those measurements, it was shown that the system behaves as a two-dimensional system and stage 5 exhibits maximum characteristics of the two-dimensional nature relative to the other stages. If the charge carriers are confined between the planes, one would expect the conduction along the c axis to be minimum and thus the resistivity in this direction should rise. The observation of stage 5 as the transition stage between low- and high-stage behavior is in agreement with other observations[30] and the fact that in graphite, the semimetallic behavior is due to the interaction of atoms two layers apart, and stage 5 is the first stage which has at least one layer of graphite bounded by two others on each side.

The temperature coefficient of the resistivity versus the inverse of the stage index for the temperatures 293, 77, and 4.2 K are presented in Fig. 3. These coefficients are

TABLE I. Stage index vs the room temperature c-axis resistivity (Ω cm).

Stage	ρ ($FeCl_3$)	ρ ($SbCl_5$)	ρ (K)
2	1.1464	1.02	0.008
3	1.0786	1.42	0.015
4	0.7886	0.88	0.05
5	1.4323		0.15
9	0.6960		
∞	0.1115	0.1	0.19

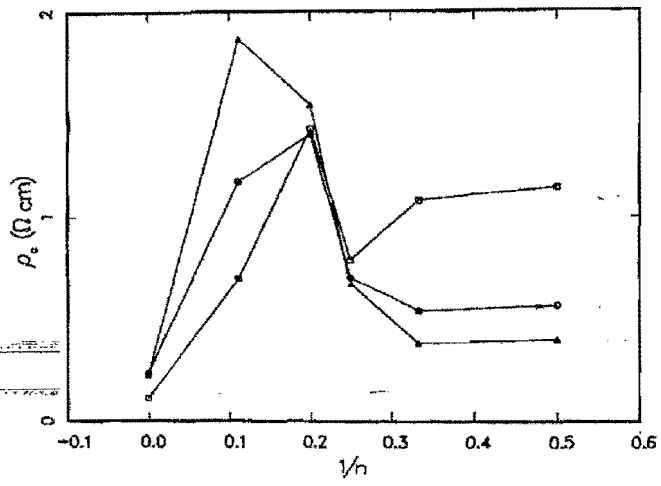

FIG. 2. c-axis resistivity vs the inverse of the stage index at room (□), liquid-nitrogen (○), and liquid-helium (△) temperatures for $FeCl_3$-GIC's and HOPG.

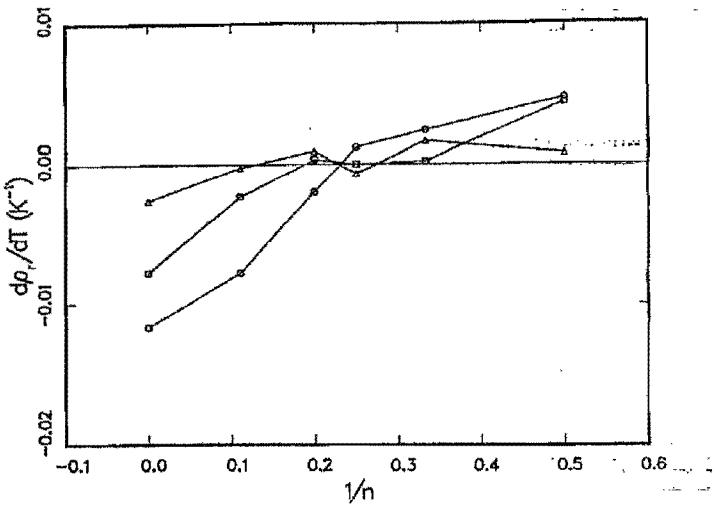

FIG. 3. Resistivity coefficient of temperature at room (□), liquid-nitrogen (○), and liquid-helium (△) temperatures vs the inverse of the stage index for stages-2, -4, -5, and -9 $FeCl_3$-GIC's, and HOPG.

the slopes of the resistivity versus temperature curves at the particular temperature normalized to the room-temperature resistivity values. This is given in units of the change of the resistivity per degree Kelvin as a fraction of the room-temperature resistivity. It is the sign of this coefficient which is important. This gives the type of temperature dependence—positive coefficients indicate "metallic" temperature behavior and negative coefficients indicate "activated" behavior. Again the fundamental difference in behavior between stages with stage index less than five and greater than five is readily apparent. Also note that for all stages the resistivity coefficient at room temperature is very nearly equal to zero.

The data in Fig. 1 were analyzed in terms of the theory of variable-range hopping conduction in parallel with band conduction. The VRHC theory was initially developed in connection with the treatment of resistivity in doped semiconductors as described by Shklovskii and Efros.[25] The hopping conductivity which forms one of the components for our data fit applies to lightly doped semiconductors. In our case we assume that the intercalant plays the part of the impurity, and the degree of compensation depends on the stage. Although the graphite is a semimetal, it looks very much like a semiconductor in the c direction, especially across an intercalant plane. In order to obtain the resistivity in this theory, one uses percolation, and the temperature dependence of the resistivity depends on many factors, including the dimensionality and compensation of the system. In this theory, the general expression for the VRHC resistivity is

$$\rho_h=\rho_0\left[\frac{T_0}{T}\right]^{n_1}\exp\left[\frac{T_0}{T}\right]^{n_2}, \tag{1}$$

where

$$T_0=\frac{\beta}{g(\mu)a^3k}. \tag{2}$$

$g(\mu)$ is the density of states at the Fermi level, a is the localization radius, k is Boltzmann's constant, and β is a numerical coefficient. In (1), T_0, n_1, and n_2 are functions of doping, compensation, and the dimensionality of the system.

The hopping conduction is assumed to be in parallel with the band conduction, for which the resistivity can be written as

$$\rho_b=\rho_c T^{n_3}+\rho_r, \tag{3}$$

where ρ_c is a constant multiplying the temperature-dependent term, n_3 is the power of the temperature, and ρ_r is the residual resistivity due to imperfections.

$$\rho=\frac{\rho_h\rho_b}{\rho_h+\rho_b}. \tag{4}$$

The lines drawn through the data points in Fig. 1 are the results of a fit of Eq. (4). Table II lists the values of the parameters in Eqs. (1) and (3) for each of the stages measured. From this table one observes several systematic variations of the constants with stage.

The parameter T_0 is small and in the range of 100 K for stages 2, 3, and 4 signifying a rather large radius of localization, and/or a large density of states at the Fermi level. In stage 5, T_0 is about 800 K while higher stages and HOPG have values of over 1000 K. This indicates that the localization radius decreases with stage, or the density of states at the Fermi level decreases. Our suspicion is that it is the localization radius which is mainly responsible for the change in T_0. If one assumes that the impurities are concentrated near the intercalant layers, the charge screening of the graphite layers becomes more effective as the stage increases. This was shown in the magnetic susceptibility measurements[3] and will be discussed further below.

TABLE II. Stage index versus variable parameters.

Stage	ρ_0	T_0	n_1	n_2	ρ_c	n_3	ρ_i
HOPG	0.006 74	1060	1.19	0.333	0.000 567	1	0.227
9r	1.27	27 800	−1.06	0.333	0.001 58	1	1.74
9r	0.131	3540	−0.121	0.333	0.000 314	1	1.86
5	2.86	796	−1.19	0.6	0.001 51	1	1.51
4	0.717	65.2	−0.075	0.6	0.005 73	1	0.645
3	0.396	64.8	−0.781	0.6	0.008 17	1	0.380
2	0.548	115	−0.85	0.6	0.007 63	1	0.369

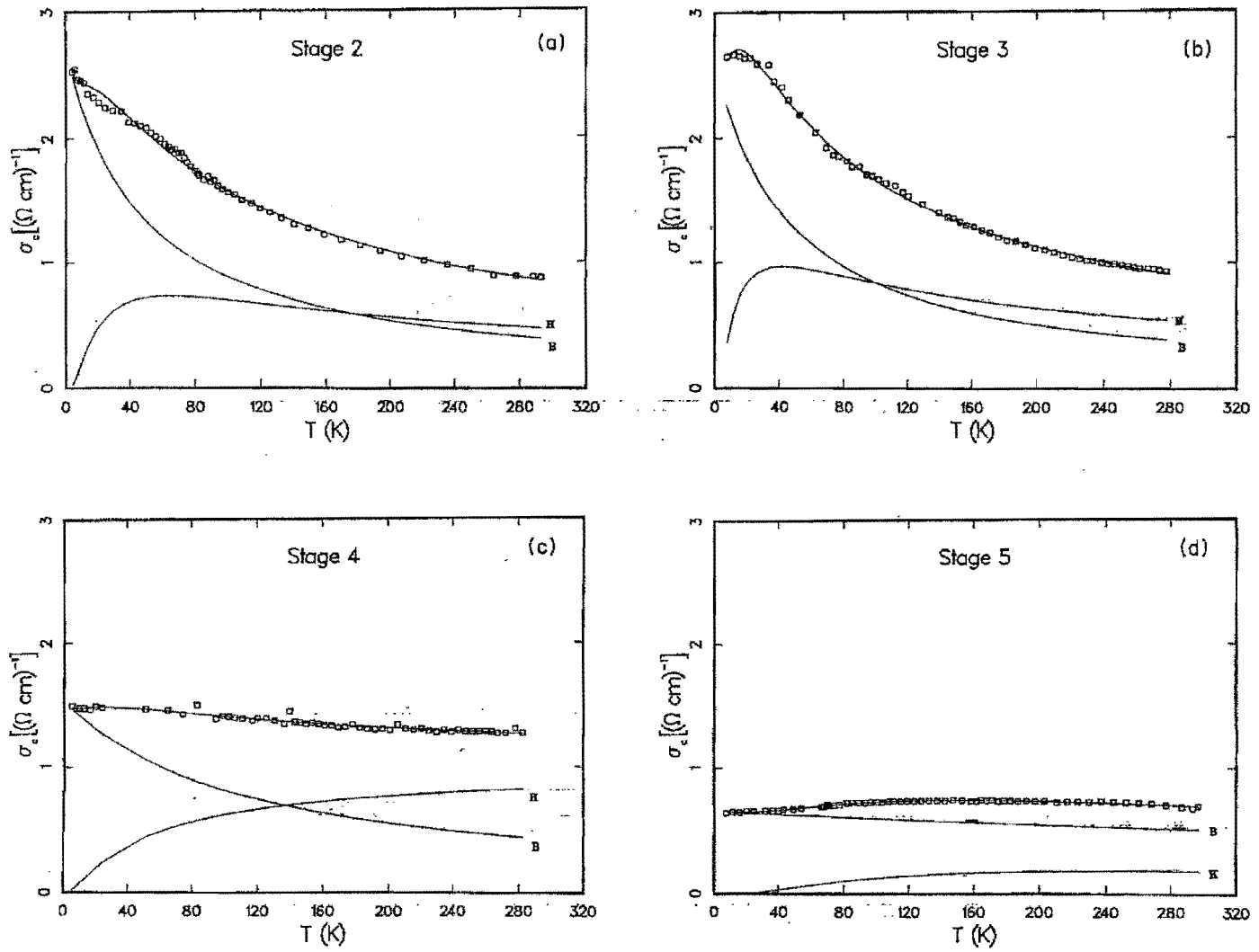

FIG. 4. The electrical conduction along the c axis for the stages indicated. The line denoting the band-conduction contribution is labeled B, while the hopping contribution is denoted by H. $9r$ is the scan-up for stage 9.

Another marked change occurs in n_2. For stages 2–5 the value of n_2 which gives the best fit to our data is 0.6, and according to the theory it is the value for a lightly doped and compensated material. That compensation leads to a Coulomb gap in the density of states at the Fermi level. Higher stages and HOPG have a value of n_2 close to $\frac{1}{3}$ which corresponds to a two-dimensional hopping-conduction mode.

In the fits shown, n_3 was held constant at a value of 1. Letting n_3 vary improved the fits only slightly. For best agreement with the data, the values of n_3 ranged from 1 to 1.8 with most below 1.4. Note that some of the in-plane resistivity measurements[11] are analyzed in terms of three components; the constant resistivity, and one with a linear and quadratic dependence on temperature. There may be a correlation between the inplane and c-axis band resistivities. There is a remarkable, almost linear dependence of the residual resistivity on stage, which implies that the number of defects in the high stages is very large, while those defects either heal or become incorporated into an orderly array in the lower stages. Such an order might imply a correlation between the intercalant layers. For HOPG the residual resistivity is small while for stage 9 it is very large. This suggests that an abundance of cracks is present between the graphite layers at the beginning of the intercalation process and that the intercalate, in high stages, might itself act as a dislocation.

The values of n_1 are somewhat harder to interpret than those of the other parameters because within VRHC its interpretation is on a more tenuous ground than that of the other parameters. In general this parameter is related to ν, the critical exponent associated with the correlation radius in the percolation theory. The value of ν is 1.34 for a two-dimensional system while in a three-dimensional system it is 0.82. For nearest-neighbor impurity hopping $n_1=-1$. For variable-range hopping $n_1=(\nu-2)/4$, while for amorphous systems, where the impurity wave functions are governed by short-range potentials, $n_1=(\nu+2)/4$. With the exception of stage 4 and 9, n_1 has a value close to -1, while in stages 4 and 9

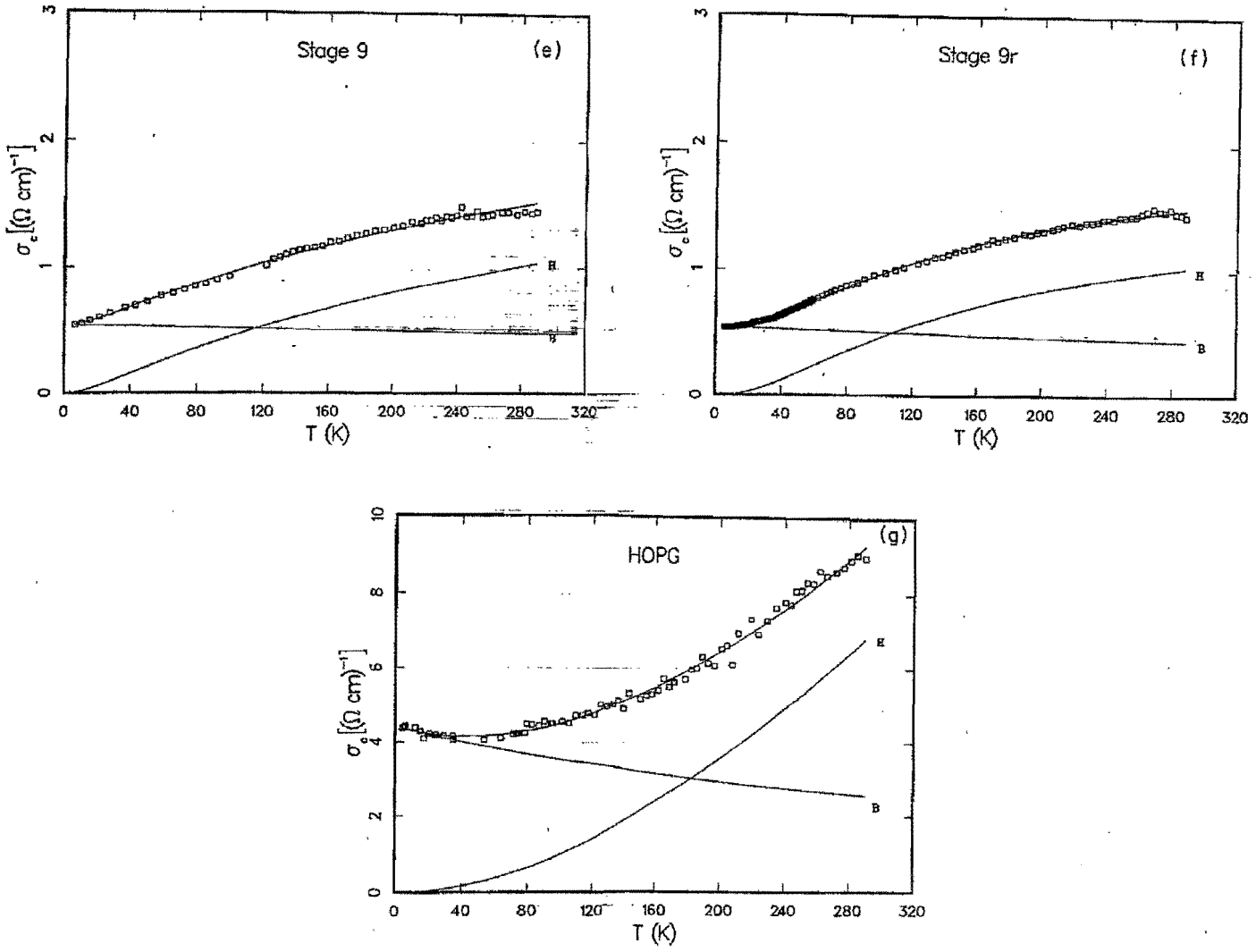

FIG. 4. (*Continued*).

the value of this parameter is closest to the two-dimensional model. The HOPG value of n_1 corresponds to that of an amorphous substance which gives credence to the interpretation of the c-axis resistivity[31] in terms of uncorrelated cracks where the impurities are trapped. We should caution the reader, however, that a lower validity should be ascribed to the physical interpretation of this parameter.

It is instructive to separate the hopping and the band contributions for each stage as a function of temperature. This is done most easily if one considers the conductivity rather than the resistivity. This is shown in Figs. 4(a)–4(g) where the conductivity of each stage, denoted by the line through the experimental points, is decomposed into the band "B" and VRHC "H" conductivities. One observes that the band conductivity dominates at low temperature in all stages. This corraborates the assumption of Ubbelohde, that in acceptor GIC's the c-axis conduction is dominated by band conduction.[32] Hopping conduction becomes comparable to or greater than band conduction only above 100 K. Stage 5 marks the transition where for lower stages band conduction is dominated by the temperature-dependent part while for stage 5 and higher the residual resistivity predominates. The hopping conductivity is the smallest in stage 5.

Because of the qualitative similarity between our data and the data of Morelli and Uher[16] we believe that their data are also amenable to a similar interpretation, where their stage 4 plays the role of the intermediate stage, similar to that of our stage 5. The data of Phan, Fuerst, and Fischer[15] might be interpreted in a similar way, although the absolute values of the c-axis resistivity of the donor compounds are smaller than those of the acceptors. In the latter set of data stage 4 plays the role of the transition stage.

The large value of the c-axis resistivity of stage 5 may be due to the delocalization of the electrons in the a-b plane as a result of its two-dimensional nature. This is accompanied by a doubling of the residual resistivity with respect to stage 4 and a large increase in T_0 which denotes the increased trapping of the impurity charge. This role of stage 5, as a boundary stage between low and high stages, is emphasized by the correlation with the magnetic susceptibility data[3] which show a susceptibility

maximum at about 1.75 K. The size of this maximum, which indicates the two-dimensional nature of this system, has an exponential dependence on the stage index. The two-dimensionality is maximum at stage 5. In Fig. 5 we plot the natural logarithm of the anisotropy (σ_c/σ_{ab}) as a function of the stage index. As shown in Fig. 5, the data for stage 2–5 follow an exponential law. On the same figure we plot the natural logarithm of the susceptibility peak, at the reported 1.75-K phase transition.[3,26] As shown, the data from two independent measurements follow the same general exponential behavior. Such exponential anisotropy dependence has been predicted by Markiewicz[22] on the basis of c-axis band conduction.

In order to see if there are any hysteretic effects, thermal cycling of the resistivity was also performed for all stages. No hysteresis was observed in any of the stages except for stage 9. The data plotted in Fig. 6 are the scan up and scan down of the c-axis resistivity versus temperature for stage 9. Although we suspect that this hysteresis might have been caused by experimental effects, we have plotted the two data sets separately in Fig. 1. The data taken with the temperature increasing after the sample was cooled is denoted in the table by stage 9r. The two scans were fitted separately to Eq. (4) with the scan up showing an increase in T_0 by a factor of the order of 10 from that of the scan down. If this effect is real, it may denote a trapping of the impurity charges at low temperatures, since according to Eq. (2) a larger T_0 denotes a smaller localization radius.

We thus conclude that, with the possible exception of stage 9, the $FeCl_3$-GIC's unlike the $SbCl_5$-GIC's, have no significant hysteresis which would be related to microscopic transition mechanisms such as the pinning of discommensurations caused by defect sites in HOPG.[16] The high-temperature order-disorder transition[33] which occurs near room temperature in stages 1 and 2 ICl-graphite intercalated compounds,[18] and that occurring in $SbCl_5$, does not exist in the $FeCl_3$-graphite compounds. The absence of the hysteresis and such high-temperature

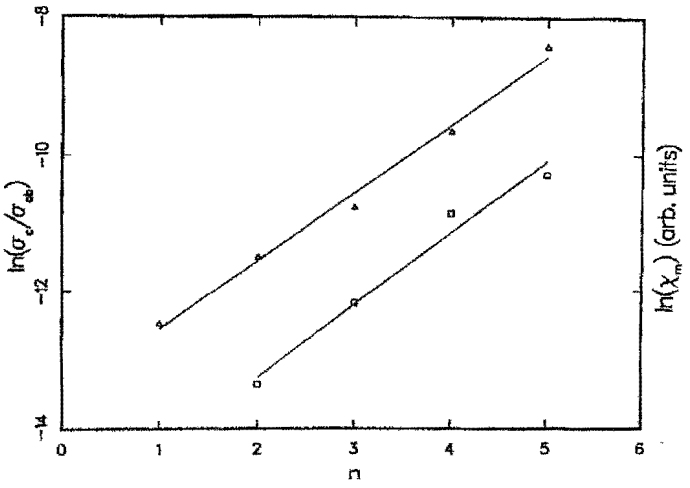

FIG. 5. Natural logarithm of the anisotropy (σ_c/σ_{ab}) (□) and the peak height of the magnetic susceptibility (△) vs stage index for $FeCl_3$-GIC's.

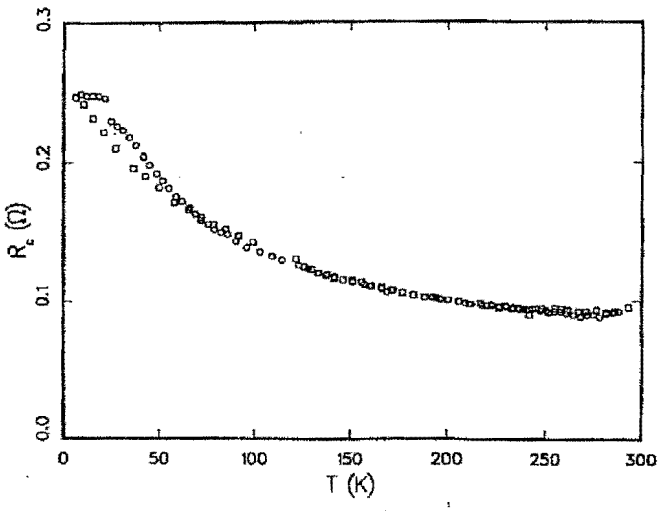

FIG. 6. Scan-up (□) and scan-down (○) of resistivity vs temperature for stage-9 $FeCl_3$-GIC.

structural phase transitions and the long period room-temperature stability suggest that the $FeCl_3$ system is a suitable candidate among the series of GIC's for further structural studies.

CONCLUSION

To date there are three comprehensive measurements[15,16] of the c-axis electrical resistivity of GIC's. Two are on acceptor compounds while the third is on a donor. As observed by McRae, Mareche, and Hérold,[17] there is the qualitative commonality in the behavior of all the c-axis resistivity measurements on GIC's. There is the typical behavior of the low stages where the resistivity increases with temperature, there is a stage which exhibits an intermediate behavior where relatively minor changes occur in the resistivity, and there is the high-stage behavior where generally the resistivity decreases with temperature. The intermediate stage can show a slight increase in the resistivity with temperature at high temperature, and a decrease at low temperature. The intermediate stage occurs at either stage 4 or 5 depending on intercalant species. In our case, the highest room-temperature resistivity was measured in the intermediate stage, stage 5. The main difference between the acceptor and donor GIC's is that the low-stage acceptors have a much greater c-axis resistivity than HOPG while the donor compound has a much smaller c-axis resistivity.

Here we have shown that the c-axis conductivity can be analyzed in terms of band conduction in parallel with variable-range hopping conduction. Band conduction dominates in all cases at temperatures below 120 K. In combination with the variable-range hopping conduction, the relation of the temperature-dependent term of the band resistivity to that of the residual resistivity is most influential in determining whether the resistivity increases or decreases with temperature. Residual resistivity increases with stage, which suggests an ordering between the intercalant planes as the distance between them

decreases. Analysis of the low-stage conduction suggests that the intercalant contributes to the band conduction in the c direction. Stage 9 in our measurements had the largest residual resistivity which might indicate that the intercalant islands form in a more random manner than those in lower stages. Also, the initiation of the intercalation process introduces cracks between the graphite planes which account for the large residual resistivity. HOPG, on the other hand has a low residual resistivity although not insignificant as compared to that of stage 2.

There may be an alternate interpretation of the data. This assumes that the mosaic spread of the graphite layers increases as the stage decreases. Since the in-plane conduction is associated with band conduction, one assumes that the band conduction along the c axis is due to the mosaic spread or the bending of the graphite planes. As the stage increases, the planes become more parallel to each other, and cracks between and parallel to the planes become the dominant contribution to the resistivity mechanism.

The parameters in the VRHC theory also illuminate the electronic structure of our material. The intercalant provides the doping of the semimetal, graphite. The impurity charges are somewhat loosely bound in the low stages, as evidenced by the low value of T_0, while in high stages the screening contributes to the stronger trapping. In the low stages there may also be a greater overlap of the impurity wave functions. The compensation in the low stages is close to one because there might be enough impurities to compensate the graphite electrons. This is also confirmed in our Hall-effect measurements where we find that at low fields the sign of the charge carriers is positive in the low-stages of $FeCl_3$-GIC's, while in the high stages the charge carriers are negative.[34] In high stages and HOPG, the conductivity is that of an uncompensated two-dimensional system. Although Tsuzuku[31] ascribes the c-axis conductivity of HOPG mainly to the in-plane band conduction around interplanar voids, the high-temperature conductivity cannot be explained without the addition of VRHC which becomes dominant above 200 K. The voids might thus form traps for charges or foreign impurities may be present in HOPG.

Finally, we conclude that the shielding of the magnetic interaction between the intercalant layers and the anisotropy in the conductivity between the c-axis and in-plane directions are correlated, and both of these effects depend on the localization of the charge carriers within the planes.

Note added in proof. Uher and Sanoler[35] described the resistivity of exfoliated graphites in terms of VRHC.

ACKNOWLEDGMENTS

We would like to acknowledge with thanks Dr. A. W. Moore for donating the HOPG, Dr. G. Dresselhaus, Dr. M. S. Dresselhaus, and Dr. K. Sugihara for many helpful discussions and preparation of initial samples. This work was supported by the U.S. Air Force Office of Scientific Research Grant No. AFOSR-82-0286.

[1]J. P. Issi, J. Heremans, and M. S. Dresselhaus, Phys. Rev. B **27**, 1333 (1983).
[2]M. Elahy, C. Nicolini, G. Dresselhaus, and G. O. Zimmerman, Solid State Commun. **41**, 289 (1982).
[3]A. K. Ibrahim and G. O. Zimmerman, Phys. Rev. B **35**, 1860 (1987).
[4]W. Metz and D. Hohlwein, Carbon **13**, 87 (1975).
[5]C. Underhill, S. Y. Leung, G. Dresselhaus, and M. S. Dresselhaus, Solid State Commun. **29**, 769 (1979).
[6]M. S. Dresselhaus and G. Dresselhaus, Adv. Phys. **30**, 139 (1981).
[7]A. R. Ubbelohde, Proc. R. Soc. London, Ser. A **327**, 289 (1972).
[8]F. L. Vogel, G. M. T. Foley, C. Zeller, E. R. Falardeau, and J. Gan, Mater. Sci. Eng. **31**, 261 (1977).
[9]G. M. T. Foley, C. Zeller, E. R. Falardeau, and F. L. Vogel, Solid State Commun. **24**, 371 (1977).
[10]L. A. Pendrys, T. C. Wu, C. Zeller, H. Fuzellier, and F. L. Vogel, in Extended Abstracts of the 14th Biennial Conference on Carbon, 1979, p. 306 (unpublished).
[11]M. E. Potter, W. D. Johnson, and J. E. Fischer, see Ref. 10, p. 300.
[12]I. L. Spain, C. Zeller, and F. L. Vogel, see Ref. 10, p. 302.
[13]E. McRae, A. Metrot, P. Willmann, and A. Herold, Physica **99B**, 541 (1980).
[14]C. Zeller, L. A. Pendrys, and F. L. Vogel, J. Mater. Sci. **14**, 2241 (1979).
[15]K. Phan, C. D. Fuerst, and J. E. Fischer, Solid State Commun. **44**, 1351 (1982).
[16]D. T. Morelli and C. Uher, Phys. Rev. B **27**, 2477 (1983).
[17]E. McRae, J. F. Mareche, and A. Hérold, Extended Abstracts on GIC, Materials Research Society Meeting, Boston, 1986 (unpublished).
[18]Y. Ohta, K. Kawamura, and T. Tsuzuku, Conference Internationale sur la Carbons, Bordeaux, 1984, p. 298 (unpublished); International Conference on Carbon, 1985 (unpublished).
[19]J. P. Issi, B. Poulaert, J. Herman, and M. S. Dresselhaus, Solid State Commun. **44**, 449 (1982).
[20]K. Sugihara, Phys. Rev. B **29**, 5972 (1984).
[21]S. Shimamura, Synth. Metals **12**, 365 (1985).
[22]R. S. Markiewicz, Solid State Commun. **57**, 237 (1986); Phys. Rev. B **37**, 6453 (1988).
[23]S. Pietronero, S. Strusler, H. R. Zeller, and M. J. Rice, Phys. Rev. Lett. **41**, 763 (1978).
[24]F. Batallan, J. Bok, I. Rosenman, and J. Melin, Phys. Rev. Lett. **41**, 330 (1978).
[25]B. I. Shklovskii and A. L. Efros, *Electronic Properties of Doped Semiconductors* (Springer-Verlag, Berlin, 1984).
[26]A. K. Ibrahim and G. O. Zimmerman, Phys. Rev. B **34**, 4224 (1986).
[27]M. R. Corson, S. E. Millman, G. R. Hoy, and H. Mazurek, Solid State Commun. **42**, 667 (1982).
[28]G. Kirczenow, Phys. Rev. B **31**, 5376 (1985).
[29]S. Hendricks and E. Teller, J. Chem. Phys. **10**, 147 (1942).
[30]J. E. Fischer, in *Intercalated Layered Materials*, edited by F. A. Levy (Reidel, Dordrecht, 1979).
[31]T. Tsuzuku, Carbon **17**, 293 (1979).
[32]A. R. Ubbelohde, Proc. R. Soc. London, Ser. A **321**, 445

(1972).
[33]K. Tashiro, M. Saito, and T. Tsuzuku, presented in the International Symposium on GIC, Tsukuba, Japan, 1985 (unpublished).
[34]A. K. Ibrahim, R. Powers, G. Zimmerman, and M. Tahar, IMMM Conference, Baltimore, 1986; J. Appl. Phys. **61**, 4382 (1987).
[35]C. Uher and L. M. Sanoler, Phys. Rev. B 27, 1326 (1983).